ISSN 1674-1056
http://cpb.iphy.ac.cn
http://iopscience.iop.org/cpb
中国物理 B
Chinese Physics
中国物理
Chinese Physics B

Enhancing von Neumann entropy by chaos in spin-orbit entanglement

Chen-Rong Liu(刘郴荣)[1], Pei Yu(喻佩)[1], Xian-Zhang Chen(陈宪章)[1], Hong-Ya Xu(徐洪亚)[2], Liang Huang(黄亮)[1], Ying-Cheng Lai(来颖诚)[2,3]

Citation: Chin. Phys. B . 2019, 28(10): 100501 . **doi:** 10.1088/1674-1056/ab3dff
Journal homepage: http://cpb.iphy.ac.cn; http://iopscience.iop.org/cpb

What follows is a list of articles you may be interested in

Chaotic analysis of Atangana-Baleanu derivative fractional order Willis aneurysm system

Fei Gao(高飞), Wen-Qin Li(李文琴), Heng-Qing Tong(童恒庆), Xi-Ling Li(李喜玲)
Chin. Phys. B . 2019, 28(9): 090501 . **doi:** 10.1088/1674-1056/ab38a4

Dynamical stable-jump-stable-jump picture in a non-periodically driven quantum relativistic kicked rotor system

Hsincheng Yu(于心澄), Zhongzhou Ren(任中洲), Xin Zhang(张欣)
Chin. Phys. B . 2019, 28(2): 020504 . **doi:** 10.1088/1674-1056/28/2/020504

Design new chaotic maps based on dimension expansion

Abdulaziz O A Alamodi, Kehui Sun(孙克辉), Wei Ai(艾维), Chen Chen(陈晨), Dong Peng(彭冬)
Chin. Phys. B . 2019, 28(2): 020503 . **doi:** 10.1088/1674-1056/28/2/020503

A novel pseudo-random coupled LP spatiotemporal chaos and its application in image encryption

Xingyuan Wang(王兴元), Yu Wang(王宇), Siwei Wang(王思伟), Yingqian Zhang(张盈谦), Xiangjun Wu(武相军)
Chin. Phys. B . 2018, 27(11): 110502 . **doi:** 10.1088/1674-1056/27/11/110502

Phase order in one-dimensional piecewise linear discontinuous map

Ru-Hai Du(杜如海), Sheng-Jun Wang(王圣军), Tao Jin(金涛), Shi-Xian Qu(屈世显)
Chin. Phys. B . 2018, 27(10): 100502 . **doi:** 10.1088/1674-1056/27/10/100502

SPECIAL TOPIC — 110th Anniversary of Lanzhou University

Enhancing von Neumann entropy by chaos in spin–orbit entanglement*

Chen-Rong Liu(刘郴荣)[1], Pei Yu(喻佩)[1], Xian-Zhang Chen(陈宪章)[1], Hong-Ya Xu(徐洪亚)[2], Liang Huang(黄亮)[1,†], and Ying-Cheng Lai(来颖诚)[2,3]

[1] School of Physical Science and Technology, and Key Laboratory for Magnetism and Magnetic Materials of MOE, Lanzhou University, Lanzhou 730000, China

[2] School of Electrical, Computer, and Energy Engineering, Arizona State University, Tempe, AZ 85287, USA

[3] Department of Physics, Arizona State University, Tempe, AZ 85287, USA

(Received 31 July 2019; revised manuscript received 21 August 2019; published online 11 September 2019)

For a quantum system with multiple degrees of freedom or subspaces, loss of coherence in a certain subspace is intimately related to the enhancement of entanglement between this subspace and another one. We investigate intra-particle entanglement in two-dimensional mesoscopic systems, where an electron has both spin and orbital degrees of freedom and the interaction between them is enabled by Rashba type of spin–orbit coupling. The geometric shape of the scattering region can be adjusted to produce a continuous spectrum of classical dynamics with different degree of chaos. Focusing on the spin degree of freedom in the weak spin–orbit coupling regime, we find that classical chaos can significantly enhance spin–orbit entanglement at the expense of spin coherence. Our finding that classical chaos can be beneficial to intra-particle entanglement may have potential applications such as enhancing the bandwidth of quantum communications.

Keywords: spin–orbit entanglement, chaos, von Neumann entropy, spin decoherence

PACS: 05.45.Mt, 71.15.Rf, 73.23.–b **DOI:** 10.1088/1674-1056/ab3dff

1. Introduction

Quantum entanglement, the intercorrelation among different subsystems or distinct degrees of freedom of a system, is foundational to quantum mechanics and fundamental to quantum information science and technology.[1] From the point of view of quantum–classical correspondence, entanglement has no classical counterpart. However, the nature of the classical dynamics can still have some impact on quantum entanglement.[2–16] While vast knowledge has been accumulated in the field of quantum chaos that studies the manifestations of classical chaos in the corresponding quantum system,[19–21] the interplay between chaos and quantum entanglement remains to be a fundamental and fascinating topic in contemporary physics.[2–16] Typically, entanglement is referred to the intercorrelation among different subsystems, e.g., between two particles (electrons or photons) of an entangled pair. Meanwhile, the entanglement of distinct degrees of freedom of a single particle has also been discussed and demonstrated experimentally.[7,22–27] The purpose of this paper is to investigate the interplay between chaos and intra-particle quantum entanglement that can be characterized, e.g., by the von Neumann entropy between the spin and the orbital degrees of freedom of a single electron. This problem is highly relevant to spintronics and spin-based quantum computing/communication technologies. Our finding is that chaos can enhance intra-particle quantum entanglement.

Historically, the concept of quantum entanglement was originated from the Einstein–Podolsky–Rosen (EPR) paradox[28] and Schrödinger's cat.[29] The phenomenon of quantum entanglement is counterintuitive as it entails nonlocal properties of physical processes[8,11,30–33] and plays an important role in the foundation of quantum mechanics. Various aspects of quantum entanglement such as characterization, detection, and control have been actively investigated,[32] with significant applications in quantum teleportation,[34] quantum searching algorithms,[35] quantum communication[32,36,37] and computing.[32]

Quantum entanglement is intimately related to the concept of quantum coherence based on the principle of superposition of quantum states.[11,31,38] When a state ψ is composed by two coherent states ψ_1 and ψ_2: $\psi = \psi_1 + \psi_2$, one has $|\psi|^2 = |\psi_1|^2 + |\psi_2|^2 + 2\mathrm{Re}(\psi_1^* \psi_2)$, where the cross term characterizes the coherence and can be observed through interference. The presence of a detector of certain resolution[11,38] will degrade and even destroy the interference pattern and, consequently, coherence. Remarkably, the detector can generate entanglement between the detecting and the object systems,[8,11,30–32] leading to decoherence of the state of the object systems.[8,11,31,39–42] Indeed, the study of decoherence

*Project supported by the National Natural Science Foundation of China (Grant Nos. 11775101 and 11422541) and the US Office of Naval Research (Grant No. N00014-16-1-2828).

†Corresponding author. E-mail: huangl@lzu.edu.cn

© 2019 Chinese Physical Society and IOP Publishing Ltd

and entanglement constitutes an important branch of modern quantum mechanics.[8,11,30,33,43–45]

There were some previous studies of the role of classical chaos in entanglement and decoherence.[2,5–8,10–13,17,18] For example, the issue of decoherence in classically chaotic systems was investigated in terms of the Lyapunov exponent,[5,6,10,12] where an implicit relation between the purity or coherence of the quantum state and the Lyapunov exponent was obtained in the semiclassical limit.[12] The exponent was shown[12] to be effectively the decay rate of the degree of coherence, i.e., chaos is more effective at reducing coherence, suggesting that the nature of the classical dynamics plays a determining role in decoherence, regardless of the environment. The inter-relation between decoherence and entanglement then suggests that chaos might be able to enhance entanglement.[3,4,9,13] For a classically chaotic system, the simultaneous loss of coherence of certain degree of freedom and the gain of its entanglement with other degrees of freedom of the system were demonstrated.[11] In optomechanics, it was shown that complicated nonlinear dynamical behaviors can enhance quantum entanglement.[14]

Our investigation of the interplay between chaos and spin–orbit entanglement was motivated by two considerations. Firstly, manipulating the spin degree of freedom is the base of spintronics (a major class of energy efficient electronics[46,47]), the development of which often relies on a good understanding of spin transport[46–48] in mesoscopic solid state devices such as quantum dots.[49] In the mesoscopic regime, both classical and quantum behaviors are relevant, and previous works showed that different types of classical dynamics can have characteristically different effects on the electronic transport phenomena such as conductance fluctuations.[50–62] Thus, while spin is a quantum variable with no classical counterpart, in mesoscopic systems the nature of classical dynamics would have effects on quantum behaviors that involve spin due to the spin–orbit interaction.[63] Secondly, while there were previous studies on the role of classical chaos in spin transport[63–67] and entanglement between the spin and orbital degrees of freedom,[23,25,31,32,68] the interplay between chaos and intra-particle entanglement has not been investigated. Addressing this issue may lead to insights into spin-based quantum computing or quantum information technologies.

In this paper, we study spin–orbit entanglement in two-dimensional mesoscopic systems with a focus on the role of classical chaos in intra-particle entanglement. For simplicity, we study entanglement between the spin and orbital degrees of freedom of an electron in quantum-dot systems that can be chaotic in the classical limit. The underlying physical mechanism for the spin–orbit entanglement is Rashba spin–orbit coupling.[68–75] The two-dimensional quantum dot is chosen to be a cosine cavity whose classical dynamical properties can be controlled by continuously varying its length parameter.[56] To be systematic, we study nine system configurations with various degrees of chaos as characterized by the phase space structure and the maximum Lyapunov exponent. The main finding is that, in the weakly Rashba spin–orbit coupling regime, chaos can significantly enhance the spin–orbit entanglement. Because of the potential role of such intra-particle entanglement in, e.g., quantum teleportation and communication,[76,77] our result points at the advantage of exploiting classical chaos in these applications.[25,27]

It is worth emphasizing the difference between the present work and our previous works on the role of chaos in spin transport. In particular, in Ref. [67], we studied graphene quantum dots subject to unpolarized injection and examined how chaos can induce spin polarization. In Ref. [63], we considered semiconductor two dimensional electron gas (2DEG) cavities with polarized injection and investigated the circumstances under which classical chaos would preserve or destroy spin polarization. In the present work, we address the role of chaos in spin–orbit entanglement, a kind of entanglement between the internal degrees of freedom of a single particle, which can be exploited to enhance the transmission bandwidth in quantum communication. This type of intra-particle entanglement has been studied but mostly in photonic systems.[7,22–27] In solid state systems, one relevant work[68] treated the interplay among time-reversal symmetry, entanglement, and weak-(anti)localization quantum correction to conductance. While the setting of this work is chaotic quantum dots, the issue of the effect of chaos on intra-particle entanglement is not touched. The results in our present work reveal that chaos is capable of distributing scattering electrons into different transmission channels (transverse modes), leading to an enhancement of the spin–orbit entanglement at the expense of spin polarization. To the best of our knowledge, our work has uncovered the beneficial role of chaos in enhancing intra-particle entanglement.

2. Classical dynamics and Rashba Hamiltonian

We consider two-dimensional mesoscopic quantum dot type of systems. An exemplary system consists of a central cavity (scattering region) and a number of electronic waveguides (or leads) connected to the cavity. To generate a wide range of classical dynamical behaviors, we choose the cavity to have a cosine shape,[56,58,78,79] in which the whole spectrum of classical dynamics from integrable to mixed dynamics and finally to fully developed chaos can be arisen through continuous tuning of a geometric parameter of the system. In particular, the cavity region D is defined by the boundaries $x = 0$, $x = L$, $y = 0$, and $y = W + (M/2)[1 - \cos(2\pi x/L)]$. To be concrete, we assume there are two leads attached to the cavity: one on the left and the other on the right side. The nature of the

classical dynamics is determined by the values of the parameter ratios[56] M/L and W/L. For example, for $M/L = 0.11$ and $W/L = 0.18$, the classical phase space is mixed with the coexistence of Kolmogorov–Arnold–Moser (KAM) tori and chaotic regions. For $M/L = 0.22$ and $W/L = 0.36$, there is fully developed chaos without any stable periodic orbit.

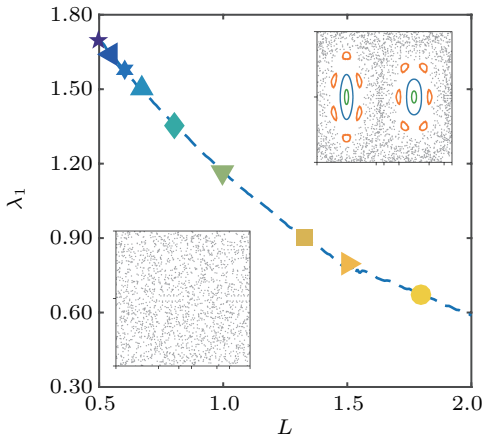


Fig. 1. Lyapunov exponent of the chaotic component in the cosine cavity. The dashed curve is the maximal Lyapunov exponent λ_1 versus the length L of the cavity. The insets are two representative Poincaré surfaces of section of the closed billiard system without leads attached to it: mixed dynamics for $L = 1.8$ μm (upper right) and chaotic dynamics for $L = 0.5$ μm (lower left). Altogether nine cases of different values of L are shown: $L = 0.5, 0.55, 0.6, 0.67, 0.8, 1.0, 1.33, 1.5, 1.8$ μm. Other parameters are $M = 0.15$ μm and $W = 0.24$ μm.

In our simulations, we fix $M = 0.15$ μm, $W = 0.24$ μm (also the width of the leads), and vary L in the range from 0.5 μm to 2.0 μm so as to generate classical dynamics with different degrees of chaos. In particular, for a closed cosine billiard system, as the length L is altered, the degree of chaos in the classical dynamics can be modulated in a continuous fashion. There are two aspects in the evolution of chaos: the chaotic component in the phase space that can increase in size (accompanied by a simultaneous decrease in the regular KAM component) and the maximum Lyapunov exponent λ_1 that can be calculated conveniently in the Birkhoff coordinates.[80] Figure 1 shows λ_1 versus L and representative phase space structures revealed on the Poincaré surface of section. For the four cases with $L \leq 0.67$, there is fully developed chaos without any stable periodic orbit in the phase space. For the five cases with $L \geq 0.67$, the phase space is mixed.[56]

To activate the Rashba spin–orbit interaction, we apply an electrical field perpendicular to the cavity plane. The Hamiltonian of the system is given by[81]

$$\hat{\mathcal{H}} = \frac{\hat{\boldsymbol{p}}^2}{2m^*}\sigma_0 + \frac{\alpha}{\hbar}(\hat{\boldsymbol{\sigma}} \times \hat{\boldsymbol{p}})_z + V_{\rm conf}(\boldsymbol{r}), \tag{1}$$

where σ_0 is the 2×2 unit matrix, $\hat{\boldsymbol{\sigma}} = (\hat{\sigma}_x, \hat{\sigma}_y)$ are the Pauli matrices, m^* is the electron's effective mass, and α is the strength of Rashba spin–orbit coupling. The confinement potential is $V_{\rm conf}(\boldsymbol{r}) = 0$ if $\boldsymbol{r} \in D$ and $V_{\rm conf}(\boldsymbol{r}) = \infty$ otherwise.

3. Characterization of spin–orbit entanglement and role of classical chaos in enhancing entanglement

For the open billiard system with leads attached to it, propagating or conducting channels will be activated when the electron Fermi energy $\varepsilon_{\rm f}$ is larger than the cut-off energy of the dispersion relation.[49] Consider the case of two symmetric leads, one on the left and the other on the right side of the scattering region, where the transport direction is from left to right. Suppose there are a number of channels in the left lead, each associated with spin-up states. The incoming orbital and spin states in the left lead are denoted as $|n\rangle$ and $|\sigma = \uparrow\rangle$, respectively. The outgoing states are in the right lead. In general, the incoming and outgoing states can be written as[82]

$$|{\rm in}\rangle = |n\rangle \otimes |\uparrow\rangle, \tag{2}$$

$$|{\rm out}\rangle = \sum_{n',\sigma'} t_{n'n,\sigma'\uparrow} |n'\rangle \otimes |\sigma'\rangle, \tag{3}$$

where the square modulus of the expansion coefficients $t_{n'n,\sigma'\uparrow}$ gives the probability for a spin-up incoming channel $|n\rangle$ from the left lead to scatter into a spin-σ' channel $|n'\rangle$ state in the right lead. That is, for any incoming state as defined in Eq. (2), equation (3) gives the corresponding state after scattering. The resulting outgoing state in the right lead is a pure but nonseparable, entangled state.[8,11,30,32,33,41–43] Associated with the outgoing state, the quantum spin and orbital degrees of freedom are thus entangled.[32,41,42,76]

When N channels are activated in the left lead, the incoming state vector can be written as the following superposition state:

$$|\psi_{\rm in}\rangle = \frac{1}{\sqrt{N}} \sum_n |n\rangle \otimes |\uparrow\rangle. \tag{4}$$

The corresponding state in the right channel after scattering is

$$|\psi_{\rm out}\rangle = C \sum_n \sum_{n',\sigma'} t_{n'n,\sigma'\uparrow} |n'\rangle \otimes |\sigma'\rangle. \tag{5}$$

With the normalization condition $\langle\psi_{\rm out}|\psi_{\rm out}\rangle = 1$, we obtain the normalization coefficient as

$$C = \frac{1}{\sqrt{\sum_{\sigma'} {\rm Tr}(\boldsymbol{t}_{\sigma'\uparrow} \boldsymbol{t}^{\dagger}_{\sigma'\uparrow})}}.$$

And the outgoing state can be written as

$$|\psi_{\rm out}\rangle = \frac{1}{\sqrt{\sum_{\sigma'} {\rm Tr}(\boldsymbol{t}_{\sigma'\uparrow} \boldsymbol{t}^{\dagger}_{\sigma'\uparrow})}} \sum_n \sum_{n',\sigma'} t_{n'n,\sigma'\uparrow} |n'\rangle \otimes |\sigma'\rangle, \tag{6}$$

where $\boldsymbol{t}_{\sigma'\uparrow}$ is the transmission matrix for all orbital channels from the spin-up state in the left lead to the spin-σ' state in the right lead, whose dimension is determined by the total number N of the conducting channels. In general, the transmission matrix can be calculated from the Green's function formalism.[82,83] Note that $|\psi_{\rm out}\rangle$ is a pure-state superposition,

which is different from a "real" mixed state.[8,11] The outgoing state is thus still a pure state, but it is entangled. In the case where there is only one propagating mode, the state becomes a product state that is separable.

The density matrix associated with the outgoing state is

$$\hat{\rho} = |\psi_{\rm out}\rangle\langle\psi_{\rm out}| = \frac{1}{\sum_{\sigma'}{\rm Tr}(\boldsymbol{t}_{\sigma'\uparrow}\boldsymbol{t}^{\dagger}_{\sigma'\uparrow})} \times \sum_{n}\sum_{n',n''}\sum_{\sigma',\sigma''} t_{n'n,\sigma'\uparrow}t^{*}_{n''n,\sigma''\uparrow}|n'\rangle\langle n''|\otimes|\sigma'\rangle\langle\sigma''|. \quad (7)$$

The reduced density matrix for the spin degree of freedom can be obtained by averaging out the total density matrix over the orbital subspace, leading to the spin density matrix that describes the spin subspace from which an observer can get the information about the system including entanglement.[11,30,32,33] Specifically, the spin density matrix is given by[8,81–84]

$$\hat{\rho}_{\rm s} = {\rm Tr}_{\rm orbital}[\hat{\rho}] = \sum_{\sigma',\sigma''}\frac{{\rm Tr}(\boldsymbol{t}_{\sigma'\uparrow}\boldsymbol{t}^{\dagger}_{\sigma''\uparrow})}{\sum_{\sigma'}{\rm Tr}(\boldsymbol{t}_{\sigma'\uparrow}\boldsymbol{t}^{\dagger}_{\sigma'\uparrow})}|\sigma'\rangle\langle\sigma''|. \quad (8)$$

Note that, the reduced spin density matrix no longer corresponds to a pure state,[8,31,83] with which the degree of mixture or reduction in coherence[11] of the remained spin state can be quantified by the purity $\mathcal{P} = {\rm Tr}[\hat{\rho}_{\rm s}^2]$, a measure of the pureness of the state. The amount of spin–orbit entanglement can be quantified by the von Neumann entropy[8,11,30–33]

$$S = -{\rm Tr}[\hat{\rho}_{\rm s}\ln\hat{\rho}_{\rm s}] = -\sum_{i}\lambda_i\ln\lambda_i,$$

where λ_i's are the eigenvalues of the reduced density matrix.

For a spin-1/2 particle, the spin density matrix can be expressed[31,81–83] in terms of the spin polarization vector $\boldsymbol{P}$. The reduced density matrix in Eq. (8) can thus be expressed as

$$\hat{\rho}_{\rm s} = \frac{\mathbf{1}+\boldsymbol{P}\cdot\hat{\boldsymbol{\sigma}}}{2} = \frac{1}{2}\begin{pmatrix} 1+P_z & P_x-{\rm i}P_y \\ P_x+{\rm i}P_y & 1-P_z \end{pmatrix}, \quad (9)$$

where $\boldsymbol{P}$ is defined as[82,83,85]

$$\boldsymbol{P} = \langle\hat{\boldsymbol{\sigma}}\rangle = {\rm Tr}[\hat{\rho}_{\rm s}\hat{\boldsymbol{\sigma}}].$$

We then have

$$\boldsymbol{P} = \sum_{\sigma'\sigma''}\frac{{\rm Tr}(\boldsymbol{t}_{\sigma'\uparrow}\boldsymbol{t}^{\dagger}_{\sigma''\uparrow})}{\sum_{\sigma'}{\rm Tr}(\boldsymbol{t}_{\sigma'\uparrow}\boldsymbol{t}^{\dagger}_{\sigma'\uparrow})}\langle\sigma''|\hat{\boldsymbol{\sigma}}|\sigma'\rangle. \quad (10)$$

The spin density matrix in Eq. (9) is obtained by tracing over the orbital part of the composite spin-orbit state $|\psi_{\rm out}\rangle$. Because the spin density matrix possesses positive eigenvalues (due to the non-negativeness of probability), the positive determinant $\det[\rho_{\rm s}] \geq 0$ leads to the condition $0 \leq |\boldsymbol{P}| \leq 1$. Since the purity associated with Eq. (9) is

$$\mathcal{P} = {\rm Tr}[\hat{\rho}^2] = (1+|\boldsymbol{P}|^2)/2,$$

information about the coherent motion of the spin state is encoded into the rotation of $\boldsymbol{P}$, and the decay of spin coherence will lead to $|\boldsymbol{P}| < 1$.[82,83] This means that $\boldsymbol{P}$'s magnitude $|\boldsymbol{P}|$ can be effectively an indicator of the purity or the coherence of the spin state. In particular, $|\boldsymbol{P}| = 1$ indicates that this spin state is completely polarized and pure and $\boldsymbol{P}$ is a vector on the Bloch sphere, the limit at the other end $|\boldsymbol{P}| = 0$ means that this spin state is totally unpolarized. While the intermediate case $0 < |\boldsymbol{P}| < 1$ indicates that this spin state is partially polarized and incompletely mixed.[11,31] Note that in general $P_x^2 + P_y^2$ could be a better indicator of spin coherence as they correspond to the off-diagonal element of the reduced density matrix. While as illustrated in Ref. [82], for spin transport with multi-transmitting modes, the quantity $|\boldsymbol{P}|$, which describes the spin polarization of the charge current, could serve the purpose better. Furthermore, we have calculated $P_x^2 + P_y^2$, the results are consistent with $|\boldsymbol{P}|$. Thus from now on, we shall use $|\boldsymbol{P}|$ as an indicator of spin coherence.

That chaos can enhance spin–orbital entanglement can be argued, heuristically, as follows. The pair of eigenvalues of the spin density matrix can be obtained as $\lambda_{1,2} = (1 \pm |\boldsymbol{P}|)/2$, with which the van Neumann entropy can be expressed in terms of the magnitude of $\boldsymbol{P}$ as[86]

$$S = -\frac{1+|\boldsymbol{P}|}{2}\ln\frac{1+|\boldsymbol{P}|}{2} - \frac{1-|\boldsymbol{P}|}{2}\ln\frac{1-|\boldsymbol{P}|}{2}. \quad (11)$$

The degree of spin–orbit entanglement as characterized by the van Neumann entropy S is thus directly connected with $|\boldsymbol{P}|$, providing an explicit relation between coherence and entanglement. The orbital degree of freedom is thus responsible for spin decoherence, providing a mechanism through which the spin polarization is reduced.

4. Results

We employ the tight-binding approximation and the recursive scattering matrix method[87–89] to calculate the spin-resolved transmission matrix $\boldsymbol{t}_{\sigma\uparrow}$ and the spin polarization vector $\boldsymbol{P}$. In particular, we discretize the scattering region using a square lattice with the nearest hopping energy $t_0 = \hbar^2/2m^*a^2$, where a is the side length of the unit cell. The Rashba spin–orbit interaction strength is $t_{\rm so} = \alpha/2a$. For convenience, we set $2m^* = \hbar = a = 1$ so that $t_0 = 1$ and $t_{\rm so}$ becomes dimensionless. If the cavity is simply a ribbon, the spin polarization in the perpendicular z direction, denoted as P_z, exhibits periodic oscillations[90–92] with $t_{\rm so}$. The periodic behavior persists even for a ribbon cavity with rough edges in the regime of weak spin–orbit interaction, although the oscillatory behavior tends to deteriorate as the interaction strength becomes strong.[63] It is thus convenient to normalize $t_{\rm so}$ by $\tilde{t}_{\rm so}$, where $\tilde{t}_{\rm so}$ is the specific value of the spin–orbit interaction strength at which

the phase of spin polarization ratio P_z changes by π, e.g., from spin up prior to entering the cavity to spin down after exiting it.

Figure 2 shows the indicators of spin coherence and the entanglement degree versus the Fermi energy ε_f and spin–orbit coupling strength t_{so}, where panels (a) and (c) are for a completely chaotic dot as marked by ★ in Fig. 1, while panels (b) and (d) display the corresponding results but for the case of mixed classical dynamics specified by • in Fig. 1. We see that for the fully chaotic cavity, there is a large decrease in coherence as characterized by $|\boldsymbol{P}|$ and simultaneously a marked enhancement of the entanglement degree as quantified by the entropy $S(\hat{\rho}_s)$ as compared with the case with mixed dynamics. This suggests that, while both sub-band mixture and spin–orbit coupling reduce the coherence,[82] classical chaos can lead to a larger loss of coherence, as shown explicitly in Fig. 2(e). And simultaneously, there is significant enhancement of spin–orbit entanglement by chaos, as shown in Fig. 2(f).

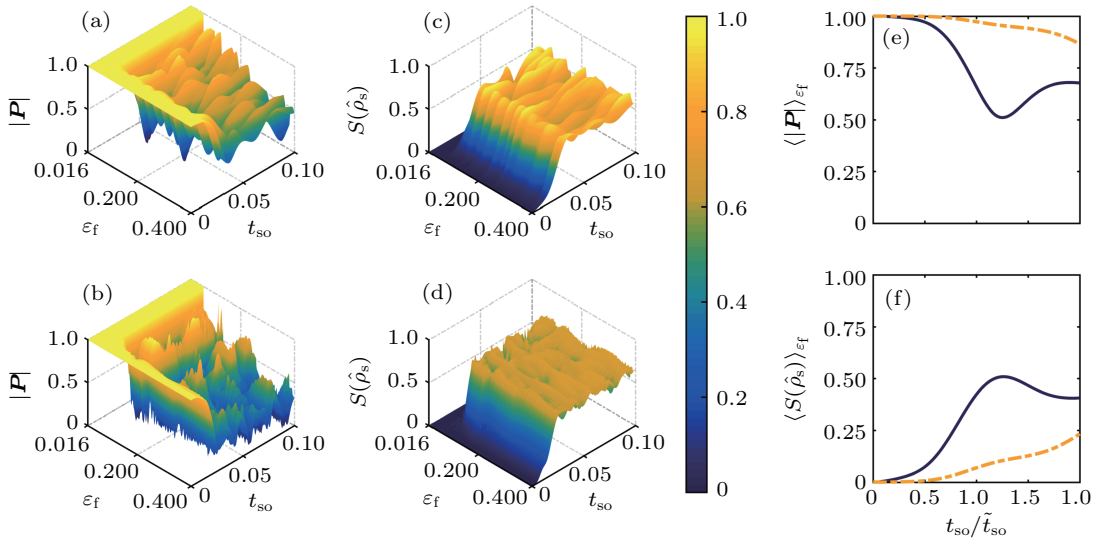


Fig. 2. Dependence of the indicators of spin coherence and the degree of entanglement on Fermi energy and spin–orbit coupling strength. (a) and (c) Three-dimensional display of the magnitude of the spin polarization vector $|\boldsymbol{P}|$ and van Neumann entropy S versus the Fermi energy ε_f and the spin–orbit coupling strength t_{so} for the cavity shape marked as ★ in Fig. 1, where the classical dynamics are fully chaotic. (b) and (d) Similar 3D plot but for the case marked as • in Fig. 1, where the classical dynamics are of the mixed type. (e) The value of $|\boldsymbol{P}|$ averaged over a relatively large interval of the Fermi energy versus t_{so} for case ★ (solid curve) and case • (dashed curve). (f) The corresponding average value of entropy S versus t_{so} for the cases in (e). Both ε_f and t_{so} are measured in units of t_0, the hopping energy of any pair of nearest sites in the square lattice as a result of discretization of the two-dimensional Schrödinger equation.

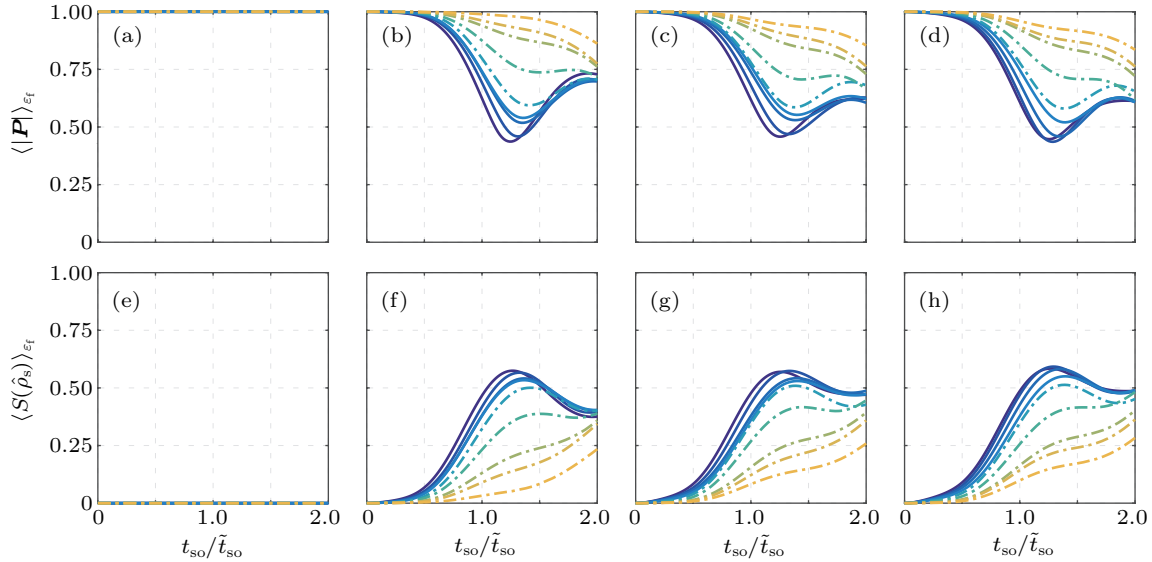


Fig. 3. Indicators of spin coherence and the degree of entanglement averaged over the Fermi energy versus the spin–orbit coupling strength. (a)–(d) Averaged magnitude of the polarization vector $\langle|\boldsymbol{P}|\rangle_{\varepsilon_f}$ and (e)–(h) averaged van Neumann entropy S versus the normalized value t_{so} of spin–orbit interaction strength for four different intervals of energy averaging: $[0.016, 0.0624]$, $[0.0632, 0.140]$, $[0.1408, 0.2472]$, and $[0.248, 0.3816]$, corresponding to regimes with one to four transmission modes, respectively. In each panel, the five dot-dashed curves are for mixed dynamics while the four solid curves correspond to chaotic dynamics.

To gain more insights into the phenomenon of enhancement of spin–orbit entanglement by classical chaos, we show in Figs. 3(a)–3(d) the value of $|\boldsymbol{P}|$ averaged over four different energy intervals, each corresponding to a distinct transport regime. The corresponding behaviors of the entropy S are shown in Figs. 3(e)–3(h), respectively. In particular, in Figs. 3(a) and 3(e), there is only one activated channel so we have $|\boldsymbol{P}| = 1$ and $S = 0$ because, in this case, the whole state in Eq. (6) is separable,

$$\begin{aligned} |\psi_{\rm out}\rangle &= \frac{1}{\sqrt{\sum_{\sigma'} |t_{11,\sigma'\uparrow}|^2}} \sum_{\sigma'} t_{11,\sigma'\uparrow} |1\rangle \otimes |\sigma'\rangle \\ &= |1\rangle \otimes \frac{1}{\sqrt{\sum_{\sigma'} |t_{11,\sigma'\uparrow}|^2}} \sum_{\sigma'} t_{11,\sigma'\uparrow} |\sigma'\rangle, \end{aligned}$$

where there is no entanglement between the spin and orbital degrees of freedom and consequently, no loss of coherence. In Figs. 3(b)–3(d) and 3(f)–3(h), more than one channel are activated. As a result, the value of $|\boldsymbol{P}|$ is reduced from the unity value, indicating a loss of coherence of the spin state and a simultaneous increase in the entropy. Indeed, insofar as the weak coupling regime $t_{\rm so}/\tilde{t}_{\rm so} \lesssim 1$ is concerned, the patterns of decrease in coherence and increase in the entanglement degree with $t_{\rm so}/\tilde{t}_{\rm so}$ as a result of classical chaos persist. If the spin–orbit interaction is too strong, the phenomena of chaos enabled coherence reduction and entanglement enhancement may not hold and the corresponding patterns may even reverse, as in this case chaos can result in enhanced spin sub-band intermixing, but with even bigger fluctuations.[63] That chaos tends to reduce coherence and directly enhances spin–orbit entanglement is consistent with previous results.[8,11,40–42] From the measurement point of view, the loss of coherence is intimately related to entanglement. Actually, the entanglement between the spin and orbital degrees is the direct reason leading to the loss of coherence of the spin state for the class of systems studied here.

5. Conclusion

For a composite quantum bipartite system with subsystems or sub-degrees of freedom,[8,11,30–33] decoherence of a subsystem and entanglement between the subsystems are intimately related.[8,11,30,33] In general, coherence is an important measure characterizing a quantum state that is the superposition of other states. When a detector is present, the quantum properties may be destroyed and the system can approach a state describable by a classical probability distribution. Our work presents an explicit demonstration of this general principle underlying coherence and entanglement in terms of spin and orbital degrees of freedom in mesoscopic electronic/spin systems with distinct types of classical dynamics. In particular, scattering into different orbital subspace leads to a nonseparable state described by a spin density matrix and loss of coherence. The entanglement for this composite system can then be studied based on the coherence of the spin subspace. For this system, reduced coherence and enhanced entanglement are thus two coexisting aspects of the same composite system.

Intuitively, classical chaos can reduce coherence in the spin polarized state through enhanced interaction between different degrees, especially through scattering into different orbital states. A question is then whether chaos can enhance entanglement. While there were previous efforts in this topic,[2,5–8,10–13] we focus on the spin–orbit entanglement, a kind of intra-particle entanglement. Using two-dimensional quantum dot systems with Rashba spin–orbit interactions as a prototypical setting, for which classical dynamics of different degrees of chaos can be readily generated, we calculate the measures of coherence and entanglement for a number of systematic cases and obtain the confirmation that, in the weakly coupling regime, chaos can significantly enhance the spin–orbit entanglement. Our result provides insights into the effect of chaos on orbital–spin hybrid entangled state, which may have potential advantages in enhancing the capacity of quantum communication based on intra-particle entanglement.[76,77,93,94]

Acknowledgment

YCL and HYX are supported by the Pentagon Vannevar Bush Faculty Fellowship program sponsored by the Basic Research Office of the Assistant Secretary of Defense for Research and Engineering and funded by the Office of Naval Research through Grant No. N00014-16-1-2828.

References

[1] Nielsen M A and Chuang I L 2000 *Quantum Computation and Quantum Information* (Cambridge: Cambridge Univ. Press)
[2] Pattanayak A K and Brumer P 1997 *Phys. Rev. Lett.* **79** 4131
[3] Furuya K, Nemes M C and Pellegrino G Q 1998 *Phys. Rev. Lett.* **80** 5524
[4] Loss D and Sukhorukov E V 2000 *Phys. Rev. Lett.* **84** 1035
[5] Jalabert R A and Pastawski H M 2001 *Phys. Rev. Lett.* **86** 2490
[6] Cucchietti F M, Dalvit D A R, Paz J P and Zurek W H 2003 *Phys. Rev. Lett.* **91** 210403
[7] Samuelsson P, Sukhorukov E V and Büttiker M 2003 *Phys. Rev. Lett.* **91** 157002
[8] Joos E, Zeh H D, Kiefer C, Giulini D, Kupsch J and Stamatescu I O 2003 *Decoherence and the Appearance of a Classical World in Quantum Theory* (Springer, Berlin Heidelberg, New York)
[9] Wang X, Ghose S, Sanders B C and Hu B 2004 *Phys. Rev. E* **70** 016217
[10] Gorin T, Prosen T, Seligman T H and Znidaric M 2006 *Phys. Rep.* **435** 33 156
[11] Schlosshauer M 2007 *Decoherence and the Quantum-To-Classical Transition* (Springer, Berlin Heidelberg, New York)
[12] Bonança M V S 2011 *Phys. Rev. E* **83** 046214
[13] Zhang H, Liu X, Shen X and Liu J 2013 *Int. J. Bifur. Chaos* **23** 1330014
[14] Wang G, Huang L, Lai Y C and Grebogi C 2014 *Phys. Rev. Lett.* **112** 110406
[15] Song L J, Wang X G, LI Y D and Zong Z G 2006 *Chin. Phys. Lett.* **23** 3190
[16] Tan J T, Luo Y R, Zhou Z and Hai W H 2016 *Chin. Phys. Lett.* **33** 070302

[17] Song L J, Yan D, Gai Y J and Wang Y B 2010 *Acta Phys. Sin.* **59** 3699 (in Chinese)
[18] Yang Y B and Wang W G 2015 *Chin. Phys. Lett.* **32** 030301
[19] Stöckmann H J 2006 *Quantum Chaos: An Introduction* (New York: Cambridge University Press)
[20] Haake F 2010 *Quantum Signatures of Chaos 3rd ed Springer series in synergetics* (Berlin: Springer-Verlag)
[21] Huang L, Xu H Y, Grebogi C and Lai Y C 2018 *Phys. Rep.* **753** 1
[22] Hasegawa Y, Loidl R, Badurek G, Baron M and Rauch H 2003 *Nature* **425** 45
[23] Karimi E, Leach J, Slussarenko S, Piccirillo B, Marrucci L, Chen L, She W, Franke-Arnold S, Padgett M J and Santamato E 2010 *Phys. Rev. A* **82** 022115
[24] Karimi E and Boyd R W 2015 *Science* **350** 1172
[25] Wang X, Cai X, Su Z, Chen M, Wu D, Li L, Liu N, Lu C and Pan J 2015 *Nature* **518** 516
[26] Feng L, Zhang M, Zhou Z, Li M, Xiong X, Yu L, Shi B, Guo G, Dai D and Ren X 2016 *Nat. Commun.* **7** 11985
[27] Wang X L, Luo Y H, Huang H L, Chen M C, Su Z E, Liu C, Chen C, Li W, Fang Y Q, Jiang X, Zhang J, Li L, Liu N L, Lu C Y and Pan J W 2018 *Phys. Rev. Lett.* **120** 260502
[28] Einstein A, Podolsky B and Rosen N 1935 *Phys. Rev.* **47** 777
[29] Schrödinger E 1935 *Math. Proc. Cambridge* **31** 555
[30] Zurek W H 2003 *Rev. Mod. Phys.* **75** 715
[31] Zeng J Y 2014 *Quantum Mechamics. Volume II. 5th edn* (Beijing: Science Press) (in Chinese)
[32] Horodecki R, Horodecki P, Horodecki M and Horodecki K 2009 *Rev. Mod. Phys.* **81** 865
[33] Streltsov A, Adesso G and Plenio M B 2017 *Rev. Mod. Phys.* **89** 041003
[34] Bennett C H, Brassard G, Crépeau C, Jozsa R, Peres A and Wootters W K 1993 *Phys. Rev. Lett.* **70** 1895
[35] Grover L K 1997 *Phys. Rev. Lett.* **79** 325
[36] Boström K and Felbinger T 2002 *Phys. Rev. Lett.* **89** 187902
[37] Hwang W Y 2003 *Phys. Rev. Lett.* **91** 057901
[38] Feynman R P and Hibbs A R 1965 *Quantum Mechanics and Path Integrals* (Boston, Massachusetts: McGraw-Hill)
[39] Cantrell C D and Scully M O 1978 *Phys. Rep.* **43** 499
[40] Streltsov A, Singh U, Dhar H S, Bera M N and Adesso G 2015 *Phys. Rev. Lett.* **115** 020403
[41] Chitambar E and Hsieh M H 2016 *Phys. Rev. Lett.* **117** 020402
[42] Streltsov A, Chitambar E, Rana S, Bera M N, Winter A and Lewenstein M 2016 *Phys. Rev. Lett.* **116** 240405
[43] Baumgratz T, Cramer M and Plenio M B 2014 *Phys. Rev. Lett.* **113** 140401
[44] Xi Z, Li Y and Fan H 2015 *Sci. Rep.* **5** 10922
[45] Cheng S and Hall M J W 2015 *Phys. Rev. A* **92** 042101
[46] Žutić I, Fabian J and Das Sarma S 2004 *Rev. Mod. Phys.* **76** 323
[47] Fert A 2008 *Rev. Mod. Phys.* **80** 1517
[48] Baltz V, Manchon A, Tsoi M, Moriyama T, Ono T and Tserkovnyak Y 2018 *Rev. Mod. Phys.* **90** 015005
[49] Datta S 1995 *Electronic Transport in Mesoscopic Systems* (Cambridge: Cambridge University Press)
[50] Lee P A and Stone A D 1985 *Phys. Rev. Lett. 55* **1622** 1625
[51] Webb R A, Washburn S, Umbach C P and Laibowitz R B 1985 *Phys. Rev. Lett.* **54** 2696
[52] Stone A D 1985 *Phys. Rev. Lett.* **54** 2692
[53] Jalabert R A, Baranger H U and Stone A D 1990 *Phys. Rev. Lett.* **65** 2442
[54] Ketzmerick R 1996 *Phys. Rev. B* **54** 10841
[55] Sachrajda A S, Ketzmerick R, Gould C, Feng Y, Kelly P J, Delage A and Wasilewski Z 1998 *Phys. Rev. Lett.* **80** 1948
[56] Huckestein B, Ketzmerick R and Lewenkopf C H 2000 *Phys. Rev. Lett.* **84** 5504
[57] de Moura A P S, Lai Y C, Akis R, Bird J P and Ferry D K 2002 *Phys. Rev. Lett.* **88** 236804
[58] Yang R, Huang L, Lai Y C and Grebogi C 2011 *EuroPhys. Lett.* **94** 40004
[59] Yang R, Huang L, Lai Y C and Pecora L M 2012 *Appl. Phys. Lett.* **100** 093105
[60] Yang R, Huang L, Lai Y C, Grebogi C and Pecora L M 2013 *Chaos* **23** 013125
[61] Bao R, Huang L, Lai Y C and Grebogi C 2015 *Phys. Rev. E* **92** 012918
[62] Lai Y C, Xu H Y, Huang L and Grebogi C 2018 *Chaos* **28** 052101
[63] Liu C R, Chen X Z, Xu H Y, Huang L and Lai Y C 2018 *Phys. Rev. B* **98** 115305
[64] Pershin Y V and Privman V 2004 *Phys. Rev. B* **69** 073310
[65] Chang C H, Mal'shukov A G and Chao K A 2004 *Phys. Rev. B* **70** 245309
[66] Akguc G B and Gong J 2008 *Phys. Rev. B* **77** 205302
[67] Ying L and Lai Y C 2016 *Phys. Rev. B* **93** 085408
[68] Frustaglia D, Montangero S and Fazio R 2006 *Phys. Rev. B* **74** 165326
[69] Rashba E I 1960 *Sov. Phys. Solid. State* **2** 1109
[70] Dresselhaus G and Dresselhaus M S 1965 *Phys. Rev. A* **140** A401
[71] Rashba E I 2000 *Phys. Rev. B* **62** R16267
[72] Gor'kov L P and Rashba E I 2001 *Phys. Rev. Lett.* **87** 037004
[73] Koga T, Nitta J, Takayanagi H and Datta S 2002 *Phys. Rev. Lett.* **88** 126601
[74] Rashba E I and Efros A L 2003 *Phys. Rev. Lett.* **91** 126405
[75] Schliemann J, Egues J C and Loss D 2003 *Phys. Rev. Lett.* **90** 146801
[76] Pramanik T, Adhikari S, Majumdar A, Home D and Pan A K 2010 *Phys. Lett. A* **374** 1121
[77] Amiri F, Rastgoo S and Golshan M 2014 *Phys. Lett. A* **378** 1985
[78] Luna-Acosta G A, Krokhin A A, Rodríguez M A and Hernández-Tejeda P H 1996 *Phys. Rev. B* **54** 11410
[79] Mendoza M and Schulz P A 2005 *Phys. Stat. Sol. (C)* **2** 3129
[80] Lin W A and Jensen R V 1997 *Phys. Rev. E* **56** 5251
[81] Souma S and Nikolić B K 2004 *Phys. Rev. B* **70** 195346
[82] Nikolić B K and Souma S 2005 *Phys. Rev. B* **71** 195328
[83] Dragomirova R L and Nikolić B K 2007 *Phys. Rev. B* **75** 085328
[84] Dey M, Maiti S K, Sil S and Karmakar S N 2013 *J. Appl. Phys.* **114** 164318
[85] Zhang Y T, Song Z F and Li Y C 2008 *Phys. Lett. A* **373** 144
[86] Safaiee R and Golshan M M 2017 *Eur. Phys. J. B* **90** 121
[87] Usuki T, Saito M, Takatsu M, Kiehl R A and Yokoyama N 1995 *Phys. Rev. B* **52** 8244
[88] Akis R, Ferry D K, Bird J P and Vasileska D 1999 *Phys. Rev. B* **60** 2680
[89] Xiao X, Chen Z, Nie W, Zhou G and Li F 2014 *J. Appl. Phys.* **115** 223709
[90] Datta S and Biswajit D 1990 *Appl. Phys. Lett.* **56** 665
[91] Mireles F and Kirczenow G 2001 *Phys. Rev. B* **64** 024426
[92] Wang J, Sun H B and Xing D Y 2004 *Phys. Rev. B* **69** 085304
[93] Sun Y, Wen Q Y and Yuan Z 2011 *Opt. Commun.* **284** 527
[94] Heo J, Hong C H, Lim J I and Yang H J 2013 *Chin. Phys. Lett.* **30** 040301